Gallery of Fluid Motion

The way bubbles gallop

Jian H. Guan [1], Saiful I. Tamim [1], Connor W. Magoon [1], Howard A. Stone [2], and Pedro J. Sáenz [1,*]

[1] *Department of Mathematics, University of North Carolina, Chapel Hill, North Carolina 27599, USA*

[2] *Department of Mechanical & Aerospace Engineering, Princeton University, Princeton, New Jersey 08544, USA*

(Received 28 May 2025; published xxxxxxxxxx)

This paper is associated with a video winner of a 2024 American Physical Society's Division of Fluid Dynamics (DFD) Gallery of Fluid Motion Award for work presented at the DFD Gallery of Fluid Motion. The original video is available online at the Gallery of Fluid Motion, https://doi.org/10.1103/APS.DFD.2024.GFM.V2684816.

DOI: 10.1103/fbdh-fnzv

Bubbles are more than fleeting pockets of air trapped in liquid: they exhibit an ever-expanding repertoire of intriguing behaviors. From da Vinci's sketches of their swirling paths to modern-day studies of their erratic dances under acoustic waves, the rich dynamics of bubbles have long captured the attention of everyday observers, engineers, and scientists alike [1–4]. When exposed to periodic sound waves, bubbles can shift from regular pulsations to rapid zigzagging, mimicking the randomness of Brownian motion [5,6]. Under sudden pressure changes, they may collapse violently, producing cavitation—intense shock waves capable of damaging solid surfaces [1,7]. In extreme cases, the implosion may become so intense that the bubble emits a spark of light [8]. Remarkably, some crustaceans have evolved to harness this bubble collapse to stun their prey [9]. In medicine, cavitation bubbles assist in shock wave lithotripsy by enhancing the fragmentation of kidney stones [10], while oscillating bubbles can be used to induce targeted vesicle deformation and lysis, enabling controlled release or disruption at the microscale [11]. Bubbles can also challenge common intuition: they may appear to violate Archimedes' principle [12], sinking against gravity in oscillating fluids [13–15], and carbonated drinks [16]. Despite centuries of explorations, new and often surprising bubble phenomena continue to emerge. One such example is the recently discovered "galloping" bubble, introduced in our recent publication [17]. Here, we showcase this new mechanism of bubble locomotion, highlighting its rich dynamics and striking visual appeal.

In our experiments [17], we demonstrate that an air bubble held by buoyancy against the top wall of a vertically vibrated chamber filled with silicone oil may spontaneously break symmetry and begin a self-propelled "gallop" along the upper boundary (Fig. 1), driven by a resonant interaction between its vibration modes. We image the bubble from the side using a high-speed camera (Phantom 410L, 1280×800 px, 1000 fps) with LED backlighting (PHLOX LEDW) for high-contrast visualization of the interface oscillations [Figs. 1(a) and (b)]. To capture the bubble's trajectory, we track its position from a top view using the same camera [Fig. 1(c)]. A color filter

*Contact author: saenz@unc.edu

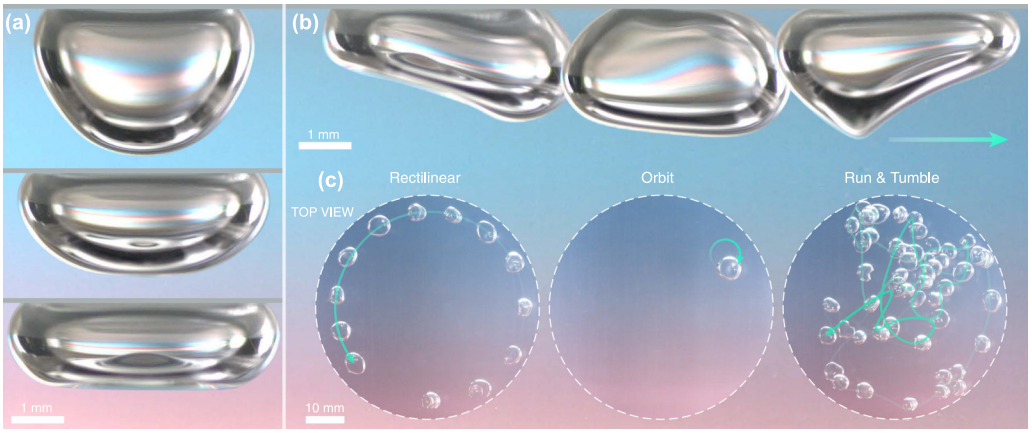

FIG. 1. Galloping bubbles. Experimental time sequences illustrating the dynamics of bubbles against the upper boundary of a vertically vibrated fluid chamber under different driving conditions. The bubble is imaged from the side in panels (a) and (b) and from the top in (c). (a) Below the galloping threshold, $A < A_G$, the bubble undergoes vertically axisymmetric shape oscillations without horizontal translation. (b) Above the galloping threshold, $A > A_G$, the bubble develops an asymmetric deformation pattern reminiscent of galloping motion and begins to self-propel. The arrow indicates the direction of motion and time. (c) Different bubble sizes and forcing parameters give rise to diverse domain exploration modes. Just above the galloping threshold, the bubble typically exhibits steady rectilinear motion (left), which curves into a circular trajectory here due to the chamber's boundary (dashed line). Depending on the bubble volume and frequency, further increasing the driving amplitude, A, may induce orbital motion (middle), or jagged paths with abrupt reorientations (right) reminiscent of "run-and-tumble" dynamics [18,19].

was placed between the backlight and the chamber to provide the background color gradient. To excite the bubble's natural modes, the fluid chamber is mounted on a vibrating table [17] and driven sinusoidally in the vertical direction, thereby inducing an effective time-varying gravitational field $G(t) = -g + A\omega^2 \sin(\omega t)$ that drives shape oscillations. Here, g is the standard gravitational acceleration, while the driving parameters are the maximum bath displacement, A, and driving frequency, $f = \omega/2\pi$. At low forcing, the bubble undergoes symmetric, harmonic shape oscillations without horizontal translation [Fig. 1(a)]. Once the driving amplitude exceeds a critical threshold, A_G, the bubble undergoes a spontaneous symmetry breaking about the vertical axis and begins to self-propel horizontally in a galloping motion [Fig. 1(b)]. In our experiments, these galloping bubbles display various domain exploration modes [Fig. 1(c)]: by tuning the bubble volume and driving parameters, the propulsion transitions between rectilinear translation [Fig. 1(c), left], orbital motion [Fig. 1(c), middle], and run-and-tumble dynamics [Fig. 1(c), right], the latter mimicking the search strategy of a variety of organisms [18,19].

We observed galloping for air bubbles immersed in silicone oil of kinematic viscosity of $\nu = 5$ cSt and characteristic size, R, comparable to the characteristic capillary length, $l_c = \sqrt{\sigma/\rho g} = 1.48$ mm, where σ is the surface tension, and ρ the liquid density. Outside this range, smaller bubbles become spherical and larger ones flatten into puddles, both of which hinder galloping. In the intermediate size range, the bubble adopts a nearly hemispherical equilibrium shape, and the emergent vibration modes closely resemble those predicted for inviscid hemispherical bubbles [20,21]. Motivated by this observation, we complement our experiments with two-phase direct numerical simulations performed in the fluid solver *Basilisk* [22] to rationalize the galloping locomotion [17]. We first simulate the galloping dynamics of bubbles similar to those in the experiments [17], which are separated from the top wall by a thin lubrication film, and observe quantitative agreement [Fig. 2(a)]. We then perform analogous simulations for hemispherical bubbles with a freely moving contact line, finding that they exhibit an analogous symmetry breaking [Fig. 2(b)]. The emergence of

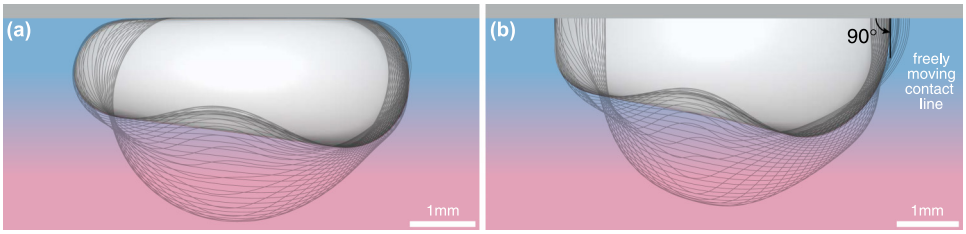

FIG. 2. Simulated galloping bubbles. Direct numerical simulations, shown here from the side, demonstrate the galloping locomotion in two distinct bubble configurations: (a) a bubble separated from the top wall by a thin lubrication film, which prevents direct contact and suppresses contact-line formation, and (b) a sessile bubble directly attached to the wall with a freely moving contact line and a 90° contact angle. The configuration in (a) corresponds to that of the bubbles in our experiments, and the simulations were performed under the same conditions and fluid properties. The configuration in (b) demonstrates that the galloping mechanism also arises in a simplified geometry, where the equilibrium bubble shape (in the absence of forcing) is hemispherical and can thus be interpreted with a minimal set of spherical harmonics. Gray lines illustrate the temporal evolution of the simulated bubble interface over a single oscillation cycle, during which the bubble self-propels a small distance to the right.

galloping in the idealized hemispherical geometry suggests that the underlying symmetry-breaking mechanism can be interpreted using a minimal set of spherical harmonics, Y_{kl}, which are specified by a polar wavenumber k and an azimuthal wavenumber l [20,21]. We perform a spectral analysis on the hemispherical galloping bubble by projecting its shape onto the subset of spherical harmonics that satisfy the no-penetration condition ($k + l =$ even). We find that axisymmetric modes, typically dominated by the amplitude of the $(2, 0)$ harmonic, are parametrically excited at low forcing, while the nonaxisymmetric mode $(3, 1)$ emerges only above the critical galloping threshold, A_G. The Reynolds number is defined using the characteristic flow speed, $u_c = A\omega$, as $\mathrm{Re} = u_c R/\nu$, which in our experiments typically falls in the range $30 < \mathrm{Re} < 50$, indicating weak viscous effects. In this inertia-dominated regime, a nonaxisymmetric mode excited in isolation would yield reciprocal oscillations without net propulsion [23,24]. Galloping bubbles overcome this constraint through a coupling between the nonaxisymmetric mode that arises above the galloping threshold ($A > A_G$) and the underlying axisymmetric oscillations, which breaks temporal symmetry and enables nonreciprocal self-propulsion [17].

We conclude by highlighting the versatility of galloping bubbles with a series of proof-of-concept experiments in Fig. 3, illustrating how the galloping instability may enable new technological advancements across diverse practical settings. The galloping instability can help dislodge and remove bubbles from nucleation sites [Fig. 3(a)], potentially offering new methods to enhance heat transfer during cooling of electronic microdevices, where trapped bubbles reduce thermal efficiency [25]. Provided the bubbles remain close or attached to the wall, as is typically the case for sessile bubbles under moderate forcing, this mechanism may be especially useful in microgravity environments, where the absence of buoyancy complicates bubble removal [26–28]. Galloping bubbles have a tendency to follow lateral walls, which enables passive, size-dependent sorting: small bubbles enter narrow collectors, while larger ones bypass them [Fig. 3(b)]. Their wall-following behavior also allows for navigation through complex mazelike environments [Fig. 3(c)], with potential applications in microfluidics and drug delivery. Additionally, galloping bubbles may offer a noninvasive cleaning method for removing microparticles from solid surfaces [29], where oscillation-induced flows beneath the bubble sweep particles downward and away from the boundary [17], showing potential as a new cleaning method for sensitive devices. We note that these applications are subject to size constraints as the galloping mechanism for film-separated bubbles relies on sizes comparable to the capillary length. By contrast, hemispherical bubbles [Fig. 2(b)] should be able to propel at

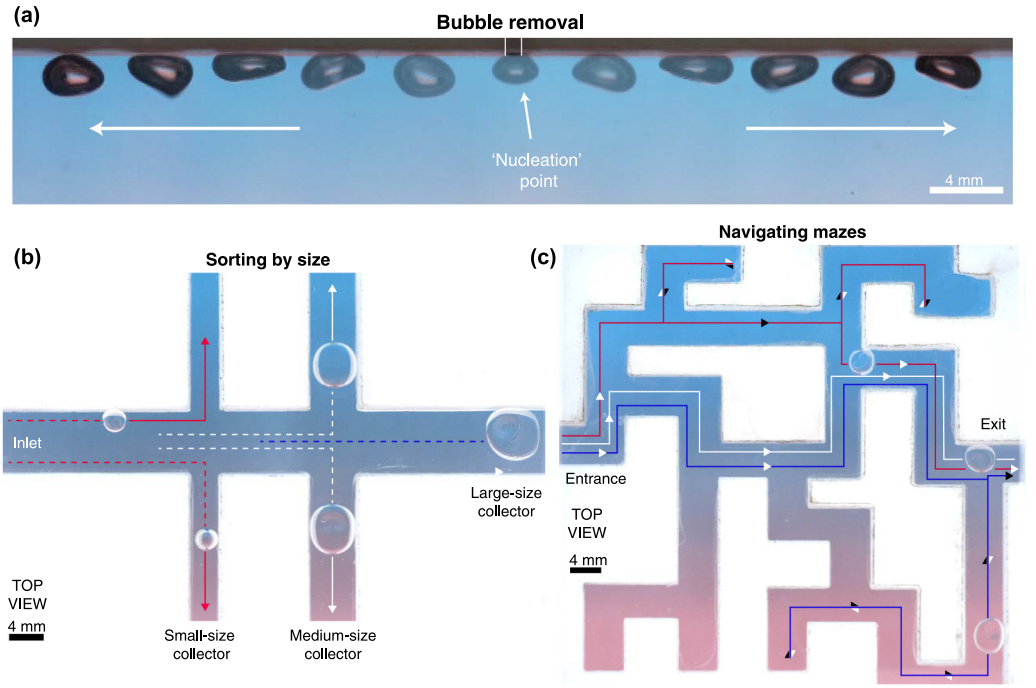

FIG. 3. Proof-of-concept applications of galloping bubbles. (a) Bubble evacuation: the galloping instability enables the removal of bubbles from a nucleation point, such as those arising during boiling processes. In this demonstration, a bubble is injected through an artificial nucleation site; once it grows to the appropriate size, the galloping instability is triggered and the bubble departs the surface autonomously, without the need for external flows or buoyancy. (b) Size-dependent sorting: owing to their affinity to adhere to and follow walls, bubbles of various volumes are autonomously directed into collectors of increasing sizes, facilitating their sorting. Shown here from a top view, bubbles released from a wide inlet channel on the left follow the sidewalls and enter the first collector whose opening exceeds their size, while larger bubbles bypass smaller collectors until reaching one of appropriate width. The galloping dynamics thus provides a robust self-sorting mechanism without the need for imposed pressure gradients or external flow control. (c) Navigation through complex networks: galloping bubbles can traverse intricate flow networks and solve mazes. Apart from their natural tendency to follow walls, galloping bubbles are also capable of reversing direction at dead ends, which enables them to autonomously find a viable path from entry to exit. This robustness demonstrates that their utility does not depend on perfectly straight channels or carefully prepared conditions, but persists in complex, irregular geometries. Colored lines and arrows trace the paths taken by different bubbles from entry to exit. Images in (a) are captured from the side, and (b) and (c) from above.

smaller scales under higher-frequency vibrations, though they may require surface treatments to prevent contact-line pinning. Significant opportunities for future research into galloping bubbles across different scales and configurations therefore lie ahead.

The authors gratefully acknowledge financial support from the National Science Foundation, under Grant CBET-2144180 (CAREER, P.J.S.), CMMI-2321357 (P.J.S. and J.H.G.), and the Alfred P. Sloan Foundation (Sloan Research Fellowships, P.J.S.).

The data supporting this study's findings are available within the article.

[1] M. S. Plesset and A. Prosperetti, Bubble dynamics and cavitation, Annu. Rev. Fluid Mech. **9**, 145 (1977).
[2] I. Marusic and S. Broomhall, Leonardo da Vinci and fluid mechanics, Annu. Rev. Fluid Mech. **53**, 1 (2021).
[3] D. Lohse, Bubble puzzles: From fundamentals to applications, Phys. Rev. Fluids **3**, 110504 (2018).
[4] D. Legendre and R. Zenit, Gas bubble dynamics, Rev. Mod. Phys. **97**, 025001 (2025).
[5] T. B. Benjamin and A. T. Ellis, Self-propulsion of asymmetrically vibrating bubbles, J. Fluid Mech. **212**, 65 (1990).
[6] Z. C. Feng and L. G. Leal, Nonlinear bubble dynamics, Annu. Rev. Fluid Mech. **29**, 201 (1997).
[7] C. E. Brennen, *Cavitation and Bubble Dynamics* (Cambridge University Press, Cambridge, 2013)
[8] M. P. Brenner, S. Hilgenfeldt, and D. Lohse, Single-bubble sonoluminescence, Rev. Mod. Phys. **74**, 425 (2002).
[9] M. Versluis, B. Schmitz, A. von der Heydt, and D. Lohse, How snapping shrimp snap: Through cavitating bubbles, Science **289**, 2114 (2000).
[10] J. E. Lingeman, J. A. McAteer, E. Gnessin, and A. P. Evan, Shock wave lithotripsy: Advances in technology and technique, Nat. Rev. Urol. **6**, 660 (2009).
[11] P. Marmottant and S. Hilgenfeldt, Controlled vesicle deformation and lysis by single oscillating bubbles, Nature (London) **423**, 153 (2003).
[12] B. Apffel, F. Novkoski, A. Eddi, and E. Fort, Floating under a levitating liquid, Nature (London) **585**, 48 (2020).
[13] R. H. Buchanan, G. Jameson, and D. Oedjoe, Cyclic migration of bubbles in vertically vibrating liquid columns, Ind. Eng. Chem. Fund. **1**, 82 (1962).
[14] V. S. Sorokin, I. I. Blekhman, and V. B. Vasilkov, Motion of a gas bubble in fluid under vibration, Nonlin. Dyn. **67**, 147 (2012).
[15] Z. Li, Y. Zhou, and L. Xu, Sinking bubbles in a fluid under vertical vibration, Phys. Fluids **33**, 037130 (2021).
[16] M. Robinson, A. C. Fowler, A. J. Alexander, and S. B. G. O'Brien, Waves in Guinness, Phys. Fluids **20**, 067101 (2008).
[17] J. H. Guan, S. I. Tamim, C. W. Magoon, H. A. Stone, and P. J. Sáenz, Galloping bubbles, Nat. Commun. **16**, 1572 (2025).
[18] O. Bénichou, C. Loverdo, M. Moreau, and R. Voituriez, Intermittent search strategies, Rev. Mod. Phys. **83**, 81 (2011).
[19] A. M. Hein, F. Carrara, D. R. Brumley, R. Stocker, and S. A. Levin, Natural search algorithms as a bridge between organisms, evolution, and ecology, Proc. Natl. Acad. Sci. USA **113**, 9413 (2016).
[20] L. Rayleigh, On the capillary phenomena of jets, Proc. R. Soc. London **29**, 71 (1879).
[21] H. Lamb, *Hydrodynamics* (Cambridge University Press, Cambridge, 1924).
[22] S. Popinet, An accurate adaptive solver for surface-tension-driven interfacial flows, J. Comput. Phys. **228**, 5838 (2009).
[23] P. G. Saffman, The self-propulsion of a deformable body in a perfect fluid, J. Fluid Mech. **28**, 385 (1967).
[24] S. Childress, *An Introduction to Theoretical Fluid Mechanics* (American Mathematical Society, Providence, RI, 2009), Vol. 19.
[25] D. E. Kim, D. I. Yu, D. W. Jerng, M. H. Kim, and H. S. Ahn, Review of boiling heat transfer enhancement on micro/nanostructured surfaces, Exp. Therm Fluid Sci. **66**, 173 (2015).
[26] V. K. Dhir, G. R. Warrier, E. Aktinol, D. Chao, J. Eggers, W. Sheredy, and W. Booth, Nucleate pool boiling experiments (npbx) on the international space station, Microgr. Sci. Technol. **24**, 307 (2012).
[27] C. Konishi and I. Mudawar, Review of flow boiling and critical heat flux in microgravity, Int. J. Heat Mass Transf. **80**, 469 (2015).
[28] S. Hong, J. Wang, Z. Gao, and C. Dang, Review on state-of-the-art research in pool and flow boiling under microgravity, Exp. Therm. Fluid Sci. **144**, 110848 (2023).
[29] S. Khodaparast, M. K. Kim, J. E. Silpe, and H. A. Stone, Bubble-driven detachment of bacteria from confined microgeometries, Environ. Sci. Technol. **51**, 1340 (2017).